Conference Paper, Published Version

Figlus, Jens; Almarshed, Badreyah

Wave Overtopping over Sand-Covered Rubble Mound Structures

Coastal Structures 2019 - Nils Goseberg, Torsten Schlurmann (eds) - © 2019 Bundesanstalt für Wasserbau
ISBN 978-3-939230-64-9 (Online) - DOI: 10.18451/978-3-939230-64-9_116

Wave Overtopping over Sand-Covered Rubble Mound Structures

J. Figlus & B. Almarshed
Department of Ocean Engineering, Texas A&M University, Galveston, Texas, United States

Abstract: The combination of hard and soft coastal risk-reduction strategies is gaining traction worldwide as a means to create multifunctional systems that can protect the hinterland from flooding via storm surge and wave attack while at the same time providing ecosystem services and pleasing aesthetics along developed coastlines. Here, such a hybrid coastal structure consisting of a rubble mound, covered by sand to simulate the look of a dune, is tested in a wave flume physical model experiment. Elevated water levels and irregular waves provided forcing conditions leading to sand profile evolution and overtopping of the hybrid structure. Three different sand layer thicknesses were compared to a structure without sand cover under various combinations of water levels and incident spectral wave heights. Through dimensional analysis, a functional relationship between the non-dimensional average overtopping rate and a non-dimensional parameter incorporating wave height, freeboard, and water depth was established. An exponential model equation was then fitted to the measured overtopping values to obtain a functional design equation for such structures that can be used for preliminary design and can be compared to traditional overtopping equations. Further studies are anticipated to verify the equation and test parameter dependencies not included in the present work.

Keywords: Hybrid structure, Rubble mound, Sand dune, Overtopping, Wave hydrodynamics, Runup, Coastal risk reduction, Morphodynamics, Design

1 Introduction

Rubble mound structures are a popular means of reducing the impact of waves on developed coastal areas and infrastructure. They are relatively easy to construct from quarry rock material and exhibit a desirable ductile failure mode due to the fact that the armor layers are comprised of individual armor units. Their rough surface, slope, and voids between rocks provide excellent wave energy dissipation characteristics which often makes them the preferred choice for nearshore breakwaters or coastal revetments.

Increasingly, coastal risk-mitigation strategies are moving toward multifunctional and hybrid approaches with nature-based components where different concepts are combined to create synergistic effects related to flood protection, ecosystem creation, recreational use, and aesthetics (e.g., Voorendt, 2017; Sutton-Grier et al., 2015; Boers, 2012). One such type of hybrid coastal structures consisting of a traditional rubble mound covered by a sand layer is being used increasingly in coastal risk-reduction schemes around the world (Basco, 1998; Irish et al., 2013; Voorendt, 2015; Boudreau et al., 2018, Nordstrom, 2018). The hybrid system investigated here looks like a coastal sand dune but combines some of the benefits of sand dunes with those of the embedded hard structure. Especially in coastal areas with limited space where natural-looking beach and dune systems are desired, but more robust coastal protection is needed, such a hybrid approach can be a viable option. To optimize the design of sand-covered rubble mounds, wave-induced runup and overtopping as well as coupled sand layer morphodynamics and sediment overwash processes need to be investigated and understood.

Almarshed et al. (2019) present an overview of such hybrid structures and point out related open research questions.

At present, no overtopping design equations for such structures exist to address questions of required freeboard, sand layer thickness, and overtopping discharge rates based on hydrodynamic forcing conditions. In current practice, the rubble mound and sand layer components are treated independently of each other when assessing the design of such structures. In order to optimize design criteria, the two components need to be looked at in a combined fashion, especially when considering overtopping calculations, since the morphodynamic evolution of the sand layer above the rubble mound during storm impact affects runup and overtopping significantly.

The research question addressed by this work is whether it is possible to establish a functional design equation similar to those offered in the coastal structures design literature (e.g., EurOtop Manual by Van der Meer et al., 2016) for the calculation of the average wave overtopping rate over a hybrid coastal structure consisting of a rubble mound covered by a sand layer taking into account the evolution of the sand layer under wave forcing. As a starting point in answering this question, a small-scale physical model experiment was performed in a moveable-bed wave flume. The following synthesizes findings from Almarshed (2019) and details preliminary results regarding average wave overtopping rates over sand-covered rubble mound structures obtained from this experiment.

2 Physical Model Experiment and Analysis Methods

A small-scale (1:18) physical model experiment was conducted in a moveable-bed wave flume. A schematic of the experiment setup is provided in Fig. 1. The chosen combination of rubble mound and sand cover was based on potential surge barrier options envisioned for the land barrier section of a coastal spine intended to reduce the risk of flood damage for the greater Houston-Galveston metropolitan area during hurricane storm surge impact. In addition, the setup features a vertical flood wall hidden inside the sand-covered rubble mound to reduce seepage flow resulting from large head differences between ocean and bay water levels. Since practical limitations on total structure height exist, overtopping is expected to occur during peak storm conditions and is investigated here. Wave overtopping rates were measured for hybrid coastal structures covered by sand layers of three different thicknesses subject to a variety of water level, wave height, and wave period conditions as outlined in Table 1. The conditions were chosen to represent extreme storm conditions where overtopping and overwash are expected but without complete inundation of the hybrid structure.

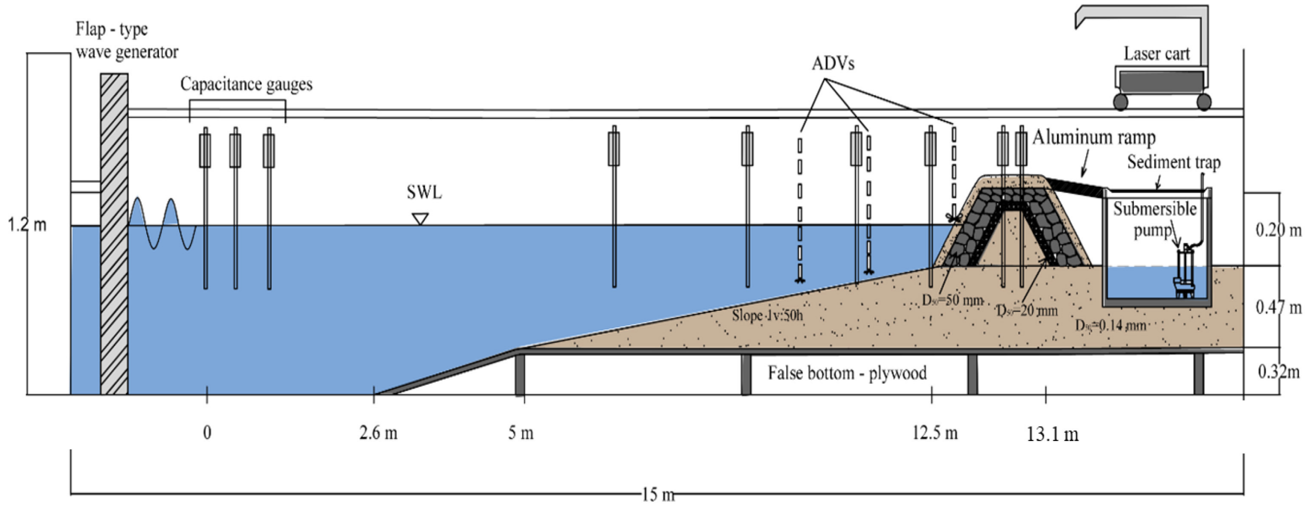

Fig. 1. Schematic cross-section of movable-bed wave flume and experiment setup (Almarshed, 2019).

The wave flume was 15 meters long, 0.6 meters wide, and 1.5 meters tall, included a beach profile made of real sand (D_{50} = 0.14 mm), and a flap-type wave maker producing irregular wave trains conforming to a JONSWAP spectral shape. The rubble mound double outer layer consisted of gravel with a nominal diameter of 20 mm on top of a finer filter layer and geotextile. An impermeable wooden board simulating the vertical flood wall was placed inside the rubble mound at the end of the horizontal crest section. The vertical wall extended to the top of the rubble mound effectively eliminating seepage through the rubble mound portion of the structure and confining overtopping flow to the sand layer and above. A total of nine capacitance wave gauges were used to measure cross-shore variations in free-surface elevation and to assess wave parameters as well as overtopping flow depth and overtopping bore progression speed over the crest of the hybrid structure. Measurements of overtopping rates over the rubble mound structure and vertical wall combination without sand cover were used as baseline comparison. Additional processes investigated in this experiment included the profile evolution of the sand layer and fronting beach during wave impact and overtopping as well as wave-induced sediment overwash over the hybrid structure.

Tab. 1. Physical Model Test Parameters

Parameter	Variable	Value*
Incident spectral significant wave height	H_{m0}	9 cm, 12 cm
Incident spectral peak wave period	T_p	1.64 s, 1.9 s
Water depth at the wave maker	h	102.3 cm, 104.3 cm
Sand cover thickness over rubble mound	S_t	0 cm, 5 cm, 7 cm, 9 cm

* Test conditions included all possible combinations of listed values (total of 32 tests).

Acoustic Doppler velocimeters and profilers were used to measure 3D water velocities near the bed approaching the hybrid structure and at its toe. A laser line scanner system recorded bed elevations in between wave runs to assess profile evolution over time. An overtopping bin connected to a flow ramp on the landward side of the structure crest at the level of the vertical wall crest allowed for overtopping volume determination. A sediment trap consisting of fine mesh fabric on top of the bin collected and separated overwashed sand from overtopped water during wave runs. Fig. 2 shows photos of the model construction process and the materials used.

The wave fields measured in the flume consisted of both incident and reflected waves. Separating the incident and the reflected waves is essential for investigating the wave-structure interactions. The incident and reflected wave energy was used to evaluate the energy dissipation of the tested hybrid structure. Low reflected wave energy values indicate higher levels of wave energy dissipation through the adjusted beach face. The measured free surface elevations from WG1 – WG3 (three gauges closest to the wave maker in Fig. 1) were used to separate the incident and the reflected spectra following the method of Mansard and Funke (1980) adapted for irregular waves over a flat bottom. The incident significant spectral wave height H_i at the toe of the structure was estimated by assuming $H_i = H_{m0}/(1+C_r)$, where H_{m0} is the total significant spectral wave height measured at the toe of the structure (sum of incident and reflected wave heights) and C_r is the estimated reflection coefficient for each wave burst. It is understood that this is only an estimate since the sediment profile during each wave butst is changing and the reflection coefficient is an average value over each respective 210-second burst. In the next step the measured incident wave heights, near the toe of the structure, were used to develop an empirical formula to estimate wave overtopping over the hybrid structure. A total of 32 tests were completed comprising all possible combinations of wave heights, water levels, and sand cover thicknesses indicated in Tab. 1. Every test contained 10 individual wave bursts of 3.5-minute (210-second) duration each.

Measuring the wave overtopping discharge was one of the main tasks in this experiment. Two types of wave overtopping discharges were calculated: the average wave overtopping rate, q, and the instantaneous wave-by-wave overtopping rate, $q(t)$, per unit length during a wave burst (3.5 min). Only results pertaining to the average wave overtopping rate, q, are presented in this paper, but for completeness, the procedure used to measure the instantaneous overtopping flow rate, $q(t)$, is given here as well. The instantaneous wave overtopping rate per unit length was calculated by multiplying the time series of the water layer thickness $h(t)$ above the structure crest and the time series of the overflow velocities $u(t)$ for the portion of the experiment where the sand cover over the crest had been eroded to avoid uncertainties created from flow through the eroding sediment layer. The time series of the water layer thickness was determined from WG9 located near the landward end of the crest (Fig. 1).

Fig. 2. Photos detailing the hybrid structure construction procedure. The sandy core of the rubble mound fronting the vertical wall (a) was covered by a geotextile fabric (b) to prevent the movement of sediment underneath the rocks. Gravel with a nominal diameter of 2 cm was used to construct the filter layer (c). Rubble mound structure before applying the sand cover (d). Finished hybrid coastal structure with sand cover of 9 cm thickness before the first wave run (e). Used materials are shown in Panel f. (Almarshed, 2019)

A reference water level (h_r) was recorded at the beginning of each wave burst (total water depth from the structure toe up to the top of an impermeable vertical wooden board terminating approximately at the top armor layer of the structure as seen in Fig. 2). This water level was then used to determine the thickness of the overtopped water layer. An overtopping event was recognized whenever the water level at WG9, $h_{WG9}(t)$, was greater than h_r. Time series of the water layer thickness $h(t)$ above the structure crest were calculated by evaluating the difference between $h_{WG9}(t)$ and h_r. In this study, a small water layer thickness was generated during most of the overtopping events. To estimate the overflow velocity during an overtopping event two wave gauges (WG8 – WG9), a known cross-shore distance of 5 cm apart, were mounted at the crest of the structure. The overflow velocities were determined using the time lag recorded by the two wave gauges resulting from a wave crest or roller front passing them in short succession. A MATLAB algorithm based on time series cross-correlation was written to detect wave fronts for each wave overtopping event and estimate the time lag. Then the time series of overflow velocities were obtained by dividing the known fixed distance between the gauges by the lag duration. The water velocity for each overtopping roller varied slightly in time and space but the bulk of the overtopped water was conveyed as part of the crest passing the vertical wall. This allowed for estimation of the instantaneous overtopping rate based on the measured wave/roller crest velocity over the vertical wall multiplied with the instantaneous water depth. Further details on this part of the experiment are beyond the scope of this paper and will be discussed in forthcoming publications.

The average wave overtopping volume per wave burst (3.5 min each) was measured by two techniques; (1) the overtopping collection basin (2) averaging instantaneous wave overtopping discharge per unit depth, $q(t)$, over time. The result of overtopping measurements consisted of 207 data points where the overtopping measurements during the first wave bursts (24 data points) of each test and several null data points (due to technical issue with a wave gauge) were excluded. To test the accuracy of the measurement technique of wave overtopping volumes, the total volumes from the collection basin and total volumes obtained from the flux measurement over the crest of the structure were compared showing very good agreement ($R^2 = 0.997$).

Here the measured average overtopping rates are used in combination with non-linear regression analysis to develop a prediction formula for overtopping of such hybrid structures. Specifically, the influence on overtopping rates of several hydrodynamic parameters including significant spectral wave height, H_{m0}, first-moment spectral period, $T_{m-1,0}$, water depth at the toe of the hybrid structure, h_t, and total structure height and freeboard, R_c, was investigated. Unlike for traditional coastal hard structures, some of these hydrodynamic and geometrical parameters are not well established for hybrid coastal structures due to the fact that the evolving sediment cover needs to be taken into account.

3 Results and Discussion

Wave overtopping rates are affected by multiple parameters including crest freeboard, the water depth at the toe of the structure, wave height, period and steepness, seaward slope of the structure, and the roughness of the structure surface (Van der Meer et al., 2016). In addition, every physical model study involving sediment and waves is subject to scale effects due to conflicting dynamic and geometric scaling laws and the difficulty in modeling prototype sand behavior without venturing into the cohesive sediment range in the model. The work presented here focusses on observed model relationships inherent to the chosen setup rather than in-depth assessment of all scale effects which are discussed in more detail by Almarshed (2019). In this experiment, only one seaward slope of 1v:2h was tested. Thus, the effect of the seaward slope is outside the scope of this study. It is noted that seaward slope may not be as important for the hybrid structures investigated here since the sand cover profile can adjust throughout a test based on equilibrium principles. The main issue to explore is the effect of the evolving sand cover layer on the measured hydrodynamics.

The initial sediment cover provided a relatively smooth slope for wave runup compared to only rubble mound material. This allowed wave runup to extend to the crest of the hybrid structure and quickly reshape the profile by moving sand material from the seaward structure slope offshore to form a submerged sand bar. This, in turn, increased wave energy dissipation as waves were now breaking over the bar further away from the hybrid structure, ultimately leading to reduced wave runup and overtopping.

While the sand cover was gradually eroded and sand material primarily moved to the offshore bar, it still took several wave bursts to expose the underlying rubble mound. During this process, the water depth at the toe of the structure changed continually as the sediment profile evolved. By tracking this evolving water depth at the toe of the structure, h_t, over the course of the experiment, the resulting overtopping data can be compared to traditional overtopping formulae which are based on fixed water depths at the toe of the structure as will be shown in the following.

It should be noted that overtopping measurements during the first wave bursts of each test were excluded from the analysis of the overtopping empirical formulation. During the first wave burst, rapid variations in crest freeboard, and water depth at the toe were encountered until the sand profile of the hybrid structure had adjusted to a geometry closer to an equilibrium profile with the incident water level and wave energy. Omitting this phase of rapid profile adjustment may also be justified due to the fact that during real storms water levels increase gradually rather than instantaneously as storm surge builds up. Thus, the profile at the height of the storm has already had some time to adjust to the new wave energy conditions.

The average wave overtopping rates were clearly dependent on the crest freeboard and varying water depth at the structure toe in this physical model study. A data set of 207 average overtopping rates was used to develop a prediction model for overtopping of hybrid structures. Using dimensional analysis, a non-dimensional average wave overtopping model was formulated:

$$\frac{q}{\sqrt{gH_{m0}^3}} = f\left(\frac{R_C}{H_{m0}}, \frac{h_t}{H_{m0}}, \frac{L_{m-1,0}}{H_{m0}}, \tan(\alpha)\right) \quad (1)$$

where q is the average overtopping rate per unit alongshore length, g is gravitational acceleration, H_{m0} is the energy-based significant wave height at the structure, R_c is the crest freeboard, h_t is the changing water depth at the toe of the structure, $L_{m-1,0}$ is the wave length determined using the ratio of spectral moments m_{-1} and m_0 at the toe of the structure, and $\tan(\alpha)$ is the initial seaward slope. The impact of $\tan(\alpha)$ on overtopping volumes was neglected as it was fixed in all experiments. Also, the effects of the third non-dimensional group listed in Eq. (1) were assumed to be minor as its values varied slightly between tests. Thus, Eq. (1) was simplified to the following expression:

$$\frac{q}{\sqrt{gH_{m0}^3}} = f\left(\frac{R_C}{H_{m0}}, \frac{h_t}{H_{m0}}\right) \quad (2)$$

In the following, the two non-dimensional groups on the right hand side of Eq. (2) are combined into one parameter since they feature the same denominator. The results using the 207 available measured average overtopping rates show that the non-dimensional average wave overtopping rate decays exponentially as the non-dimensional parameter $R_c h_t / H_{mo}^2$ increases (Fig. 3). Hence an empirical formula for the average wave overtopping rate was developed based on an exponential model equation:

$$\frac{q}{\sqrt{gH_{mo}^3}} = a \times Exp\left[-b\left(\frac{R_c h_t}{H_{mo}^2}\right)^c\right] \quad (3)$$

The three dimensionless parameters a, b, and c were determined by non-linear regression analysis to be 0.00553, 3.087, and 2.133, respectively. Comparing the measured data with predicted data obtained from Eq. (3) yields a squared correlation coefficient, R^2, of 0.72 (Fig. 3). Rearranging Eq. (3), the dimensional average wave overtopping rate q per unit alongshore length can be obtained:

$$q = 0.00553\sqrt{gH_{m0}^3} \times Exp\left[-3.087\left(\frac{R_c h_t}{H_{m0}^2}\right)^{2.133}\right] \quad (4)$$

This equation includes crest freeboard, water depth at the toe, and spectral significant wave height at the toe, but excludes structure slope, wave period, and wave length. The sand cover thickness is implicitly included via the h_t parameter since water depth at the toe varies as the sand layer evolves in time. It is noted that this relationship differs from the traditional EurOtop manual formulation to allow for inclusion of all measured test data. Both R_c and h_t depend on the changing sand cover profile and affect the average overtopping rate in a similar way. As sediment is eroded by waves to form an offshore submerged bar near the toe of the structure, the water depth h_t reduces, leading to higher discharge values. Similarly, a reduction in crest freeboard due to the eroding sediment cover also leads to higher discharge values.

This allows for comparison to traditional overtopping equations for hard structures that are often presented in a similar graphical form (e.g. van der Meer et al., 2016). For relatively small wave heights and/or large crest freeboards and water depths in front of the structure, the non-dimensional overtopping values are generally lower but also a lot more scattered as seen by measured data points with a value of $R_c h_t / H_{mo}^2 > 0.7$ on the x-axis of Fig. 3. This is expected due to the random nature of the incident waves where small variations in test conditions can easily lead to larger variations in overtopping values. For x-axis values smaller than 0.7, the non-dimensional average overtopping values follow the exponential model much closer with relatively small scatter.

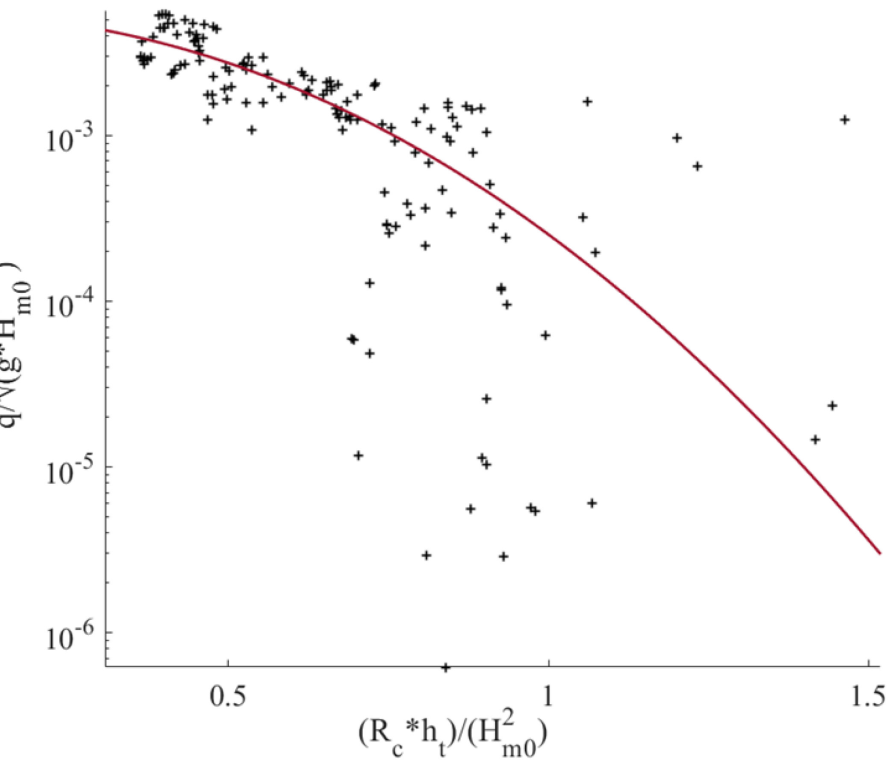

Fig. 3. Measured data (crosses) and exponential model fit (line) relating the non-dimensional average wave overtopping rate to the non-dimensional parameter including crest freeboard R_c, water depth at the toe h_t, and spectral significant wave height H_{m0} at the toe for a hybrid structure consisting of a rubble mound and varying sand cover thicknesses (R^2 = 0.72). Adapted from Almarshed (2019).

4 Summary and Conclusion

Average wave overtopping results from a small-scale physical model experiment of a hybrid coastal structure are presented. The tested hybrid structure consisted of a dual-layer rubble mound fronting an embedded vertical wall covered by sand layers of various thicknesses. Elevated water levels and irregular waves were run as 3.5-minute wave bursts forming the hydrodynamic forcing conditions for the experiment. A total of 32 tests, each with a different combination of forcing conditions and sand layer thickness and each consisting of 10 wave burst were run. The evolution of the entire sediment profile including the portion over the rubble mound was tracked via laser line scanner in between bursts. Wave overtopping rates were assessed using instantaneous water level and velocity measurements over the structure crest as well as burst-integrated water volumes collected on the landward side of the structure crest.

For the 207 valid average overtopping values obtained from the experiment, an exponential function with three fitted parameters best described the relationship between non-dimensional overtopping rate and a parameter relating crest freeboard, water depth at the hybrid structure toe, and spectral significant wave height at the structure toe ($R_c h_t/H_{mo}^2$). The fit had an R^2 value of 0.72 with a fairly distinct cut-off around $R_c h_t/H_{mo}^2$ = 0.7 where values above this threshold displayed much higher scatter in non-dimensional average overtopping rate than values below the cut-off. The dimensional equation developed from the exponential model can be used as a first step for functional overtopping design of hybrid coastal structures consisting of rubble mounds covered by sand layers of varying thicknesses. However, further physical and numerical testing is necessary to extend the range of applicability of this equation, assess scale effects, and to investigate the effects of other parameters left out in this study such as initial hybrid structure slope.

5 Acknowledgements

Dr. Almarshed was supported by a graduate fellowship from Kuwait University. Dr. Figlus and Dr. Almarshed received additional support from the National Science Foundation under Grant No. OISE-1545837.

References

Almarshed, B., 2019. Wave overtopping of hybrid coastal structures: an analysis for sand-covered rubble mounds. Ph.D. Dissertation, Texas A&M University, Texas, United States, 130 pp.

Almarshed, B., Figlus, J., Miller, J., Verhagen, H.J., 2019. Innovative coastal risk reduction through hybrid design: combining sand cover and structural defenses. Journal of Coastal Research, Coastal Education and Research Foundation, (online preprint available).

Basco, D.R., 1998. The economic analysis of "soft" versus "hard" solutions for shore protection: An example, in: Proceedings of the 26th INTERNATIONAL CONFERENCE ON COASTAL ENGINEERING. ASCE, New York, pp. 1449-1460.

Boers, M., 2012. Technisch rapport duinwaterkeringen en hybride keringen (in Dutch). Deltares, 140 pp.

Boudreau, R., Sloop, R., Holloway, A., Rivera, J., 2018. Maui’s resilient living shoreline project provides adaptation strategy for critical infrastructure. Shore & Beach, American Shore and Beach Preservation Association, 86(4), 26-35.

Irish, J.L., Lynett, P.J., Weiss, R., Smallegan, S.M., Cheng, W., 2013. Buried relic seawall mitigates hurricane Sandy's impacts. Coastal Engineering, Elsevier, 80, 79-82.

Mansard, E. P. D., Funke, E. R., 1980. The measurement of incident and reflected spectra using a least squares method, in: Proceedings of the 17th INTERNATIONAL CONFERENCE ON COASTAL ENGINEERING. ASCE, Sydney, pp. 154–172.

Nordstrom, K.F., 2018. Coastal dunes with resistant cores. Journal of Coastal Conservation, Springer, 23(1), 227-237.

Sutton-Grier, A.E., Wowk, K., Bamford, H., 2015. Future of our coasts: The potential for natural and hybrid infrastructure to enhance the resilience of our coastal communities, economies and ecosystems. Environmental Science & Policy, Elsevier, 51, 137-148.

Van der Meer, J.W., Allsop, N.W.H., Bruce, T., De Rouck, J., Kortenhaus, A., Pullen, T., Schüttrumpf, H., Troch, P., Zanuttigh, B., 2016. EurOtop: Manual on wave overtopping of sea defences and related sturctures – an overtopping manual largely based on European research, but for worlwide application (second edition), 252 pp.

Voorendt, M., 2015. Examples of multifunctional flood defences. Delft University of Technology, Delft, The Netherlands, 72 pp.

Voorendt, M.Z., 2017. Design principles of multifunctional flood defences. Doctoral Thesis, Delft University of Technology, Delft, The Netherlands, 342 pp.